Three-phase mass transfer: application of the pseudo-homogeneous and heterogeneous models

Endre Nagy[1, 2, *], Krishna D. P. Nigam[3, 4]

[1]Research Institute of Chemical and Process Engineering, Veszprem, Hungary
[2]University of Pannonia, Veszprem, Hungary
[3]Department of Chemical Engineering, New-Delhi, India
[4]Indian Institute of Technology, New-Delhi, India

Email address:
nagy@mukki.richem.hu(E. Nagy), drkdpn@gmail.com(K. D. P. Nigam)

Abstract: This paper surveyed the most important, well known two-phase mass transfer models, namely film-, film-penetration- and surface renewal models, applying them to describe the three-phase mass transfer rates at the gas-liquid interface. These models should enable the user to predict the mass transfer enhancement in the presence of a third, in the mass transport active, dispersed phase. Depending on the particle size of the dispersed phase, the pseudo-homogeneous and/or the heterogeneous model can be recommended for nanometer sized and micrometer sized particles, respectively. The effect of all important mass transport parameters, namely particle size, surface renewal frequency, diffusion depth, solubility coefficient, has been shown by typical figures. It has been analyzed how strongly depends the applicability of the homogeneous- or the heterogeneous models not only on the particle size but on the mass transport parameters. As case study, the measured and the predicted mass transfer rates have been investigated in nanofluids.

Keywords: Three-Phase Mass Transport, Heterogeneous Model, Homogeneous Model, Nanoparticles

1. Introduction

The three-phase system, with dispersed, immiscible droplets or solid particles in the liquid phase, has an important place in the engineering and chemical and biochemical fields. The effect of the dispersed phase on the absorption rate is widely investigated in research laboratories or development centers. The main objective of these studies is to predict the enhancement of the gas-liquid (or liquid-liquid) mass transfer in presence of dispersed phase. Wide variety of the three-phase system exists but this study discusses the most important mass transfer equations, applying the well-known mass transfer theories as the film-, surface renewal- and film-penetration theories, in presence of dispersed particles in the liquid boundary layer at the gas-liquid (or liquid-liquid) interface where the mass transport is not accompanied by chemical reaction in any phases. The main objective of this study is to analyze the mass transport process to be able to predict the enhancement of the absorption rate.

Recently Ramachandran[1], Kaur et al. [2] as well as Dumont and Delmas [3] survey the gas absorption in presence of dispersed phase. Ramachadran focuses his survey to show the effect of solid, reacted or catalytic particles on the absorption rate applying different physical models taken from the literature mostly utilizing the shuttle mechanism [3-10] to describe the effects of particles on the mass transfer enhancement. He does not discuss the heterogeneous model with particles freely moving in the boundary layer during the absorption. Kaur et al. [2] and Dumont and Delmas [3] summarize briefly both the homogeneous and the heterogeneous models given a few expressions to predict the enhancement. No detailed analysis of the mass transport is presented. The homogeneous models consider dimensionless, dispersed particles, which absorb/adsorb the transported component but they can be inert particles as well. Several researcher proposed and investigated the pseudo-homogeneous models [4-9] which model might only be used when the particle size is much less, about one/two orders of magnitudes less than the laminar boundary layer. This assumption is not often fulfilled when the dispersed droplet are produced by traditionally mixing process. Number of studies tries to take into account the simultaneous effect of the internal diffusion and the

continuous phase diffusion applying the more complex, one or two-dimensional heterogeneous models [10-18]. These models are recommended when the particle size is comparable, not much less, to the laminar film thickness. Both the heterogeneous and the pseudo-homogeneous models apply the mass transfer theories as film- or surface renewal theories [19] taking into account the effect of the mass transport into or through the particles being in the boundary layer.

Another approach of gas-liquid mass transport, in presence of fine solid particles as carbon particles, is considering the so-called hydrodynamic effect instead of the shuttle mechanism [20-21]. According to it the particles adsorbs the contaminants of the gas-liquid interface and due to it the liquid surface tension, and consequently the mass transfer coefficient will be changed. According to the hydrodynamic mechanism, the enhancement is induced by a transition from rigid surface to that of completely mobile one with higher mass transfer coefficient [21]. Thus, the increase in the mass transfer coefficient in presence of particles is the results in the removal of the contaminants from the interface by their adsorption onto the particles decreasing the surface tension and due to it increasing the mass transfer rate. It is obvious that this mechanism might be true in special cases, only.

The application of nanometer sized particles, or other saying, nanofuids becomes nowadays more and more important in the chemical and biochemical industries. The behavior of nanoparticles in the gas-liquid boundary layer can essentially differ from that of the micrometer sized particles. Several investigators have found that the enhancement in nanofluid can be much higher than in presence of micrometer sized dispersed phase [22-26]. Important question is how these phenomena can be explained. Krishnamurthy et al. [27] studied the diffusion of a dye and stated that its diffusion is over 10-fold higher in nanofluid than in water. Similar increase of the diffusion coefficient was obtained by Fang et al. [28] who investigated the diffusion of Rhodamine B in Cu-water nanofluid. Brownian motion of suspended nanoparticles and the induced microscopic convection of the fluids around the nanoparticles are the most important contributing factor for enhancement of the mass transport in the boundary layer. The effect of this convection on the solute diffusion coefficient could be taken into account by an additional as e.g. dispersion term in a conductive model [23, 24, 29] as it is made in heat transfer process [30]. Recently Veilleux and Coulombe proposed a Brownian motion-induced dispersion model of mass diffusion in nanofluids starting from the generalized Langevin-equation [31, 32]. This model shows a strong dependency on the particle Peclet number which causes large enhancement in the mass diffusion. The diffusion enhancement has a maximum in the ε=0 to ε=4 % volume fraction range of 10 nm Al_2O_3 nanoparticles.

2. Theory

As it has been mentioned the mathematical model of the three-phase mass transport can depend strongly on the particle (droplet) size. Basically two types of model can be recommended, namely the so called pseudo-homogeneous and the heterogeneous models. Basically, it can be stated if the particle size is comparable to the film laminar thickness or to the penetration depth of the absorbed component, the heterogeneous model is recommended for description of the mass transport in the liquid boundary layer on the gas-liquid (or liquid-liquid) interface. The pseudo-homogeneous model can only be recommended when the size of active particles (or passive ones in cases of nanosized particles, the third phase) is about one/two orders of magnitudes less than the thickness of the boundary layer or the penetration depth. The thickness of the boundary layer or the penetration depth can be easily estimated. The mass transfer coefficient can change between about 10^{-4} and 10^{-5} m/s depending on the hydrodynamic conditions. Assuming that the diffusion coefficient in the liquid phase changes between 10^{-8} and 10^{-9} m^2/s, thus the thickness can vary between about 10 μm and 100 μm by equation of $\delta = D / \beta^o$. In reality, the film thickness changes between about 10-40 μm, due to the intensive operation conditions. The penetration depth, Δy_p, can be estimated e.g. by $\Delta y_p = \sqrt{2Dt}$, where the time taken for the displacement due to diffusion is the residence time of liquid elements in the boundary layer. Let us assume that the diffusion time is equal to the reciprocal value of the surface renewal frequency according to [19], thus one can obtain that $\Delta y_p = \sqrt{2D / \beta}$, that is the penetration depth has similar values, about 10-40 μm, as the film thickness obtained by the film theory [19]. Nagy [33] compared to mass transfer results between the homogeneous and heterogeneous models in a solid, catalytic membrane layer where the spherical catalyst particles (modeled as cubic ones) were uniformly distributed in the support membrane layer. It was obtained that that the two models give similar results up to 1-3 μm with membrane thickness 30-50 μm. Accordingly, the pseudo-homogeneous model can be recommended in case of particle size about less than 1 μm and the heterogeneous model is recommended when the particle size is larger than 1 μm.

Let us look at the important mass transfer rate's equations of these models in order to be able to predict the absorption enhancement in presence of a third, dispersed phase.

In the case of the pseudo-homogeneous model the size of the dispersed phase is much smaller than the thickness of the laminar boundary layer. The particles/droplets can be regarded as dimensionless entity and they will be applied as source term in the differential mass balance equation for the boundary layer.

The boundary layer containing the dispersed phase can be illustrated by Figure 1 for the heterogeneous model. Depending on the particle size, there can be located one or more particles in the diffusion path perpendicular to the gas-liquid interface. The diffusion depth determines how

many particles (it can be more tens or even hundred), in transverse direction, can affect the gas-liquid mass transfer rate applying e.g. the surface renewal theory and thus, should be taken into account during our calculation of the mass transfer rate.

2.1. The Pseudo-Homogeneous Model

This model can be recommended when the particle size is less than 1 µm for traditional unit operations and reactors. The dispersion of a liquid phase, with droplets size less than about 1 µm, needs special methods. The preparation of nanosized solid particles is not a difficult task, nowadays. The time needed for internal diffusion ($t=R^2/D$) depends strongly on the particle size. Thus, the diffusion time of e.g. oxygen ($D_{O2}=2.3 \times 10^{-9}$ m^2/s) in a droplet with size of 50 or 1000 nm is 2.7×10^{-7} s and 4.3×10^{-4} s, respectively. The residence time of the liquid element according to the surface renewal theory ($t=D/\beta^{o2}$) is equal to 0.23 s and 23 s, for $k_L=1 \times 10^{-4}$ m/s and $k_L=1 \times 10^{-5}$ m/s, respectively. The relatively large difference between the diffusion and residence times grounds that the mass transfer in liquid nanodroplets can be considered as instantaneous. But in the case of solid, porous nanoparticles, these data can be significantly different. The diffusion coefficient can be one or two orders of magnitude less than in a liquid phase. Accordingly, the diffusion time, in solid nanoparticles, can increase up to 0.01-0.1 s, which can be comparable to that of the residence time of liquid elements in the boundary layer. Thus, the diffusion transport must not be neglected in solid nanoparticles when one describes the mass transport in the liquid boundary layer in a nanofluid. Briefly, both transport processes are discussed in the following sections.

If you want to describe the mass transport through a liquid boundary layer, first the mass transfer rate into the nanoparticles should be determined which can then be used as source term in the differential mass balance equation of the gas-liquid (or liquid-liquid) boundary layer. The differential mass balance equation for boundary layers at a planar gas-liquid (or liquid-liquid or solid liquid) interface, for unsteady-state, can be as:

$$D\frac{\partial^2 C}{\partial y^2} - J_d \frac{\omega}{1-\varepsilon} = \frac{\partial C}{\partial t} \qquad (1)$$

with initial and boundary conditions as:

if $t = 0$, $y > 0$ then $C=C^o$

if $t > 0$, $y = 0$ then $C=C^*$ (2)

if $t > 0$, $y = \delta$ then $C=C^o$

The functions J_d provides the specific mass-transfer rate into the droplets/particles in the gas-liquid boundary layer. The mass transfer rate into the dispersed phase will be defined in the next sections.

2.1.1. Mass transport rates with instantaneous internal mass transport

The J_d value cannot be given by exact value in this case. In order to solve this problem, the second term of the left hand side of Eq. (1) should be replaced by expression of $(\varepsilon/[1-\varepsilon])\ \partial C_d / \partial t$ [7]. The differential mass balance equation for the gas-liquid boundary layer will be as [23]:

$$D\frac{\partial^2 C}{\partial y^2} - \frac{\varepsilon}{1-\varepsilon}\frac{\partial C_d}{\partial t} = \frac{\partial C}{\partial t} \qquad (2a)$$

Solving the Eq. (1) with the boundary conditions given by Eqs. (2), the mass transfer rate can be given as:

$$J = \frac{D}{\delta}\frac{\lambda}{\tanh(\lambda\psi)}\sqrt{\frac{1-\varepsilon+\varepsilon H}{1-\varepsilon}}C^* \qquad (3a)$$

with

$$\psi = \lambda\sqrt{\frac{1-\varepsilon+\varepsilon H}{1-\varepsilon}}\ ; \qquad \lambda = \sqrt{\frac{s\delta^2}{D}}$$

Applying the surface renewal theory, one can get as:

$$J = \sqrt{Ds}\sqrt{\frac{1-\varepsilon+\varepsilon H}{1-\varepsilon}}C^* \qquad (3b)$$

The mass transfer enhancement can be as:

$$E \equiv \frac{J}{\sqrt{Ds}C^*} = \sqrt{\frac{1-\varepsilon+\varepsilon H}{1-\varepsilon}} \qquad (3c)$$

2.1.2. Mass Transport With Finite Internal Mass Transport

The mass balance for the inside of small particles, with initial and boundary conditions can be given as follows:

$$D_d\left(\frac{\partial^2 C_d}{\partial r^2} + \frac{2}{r}\frac{\partial C_d}{\partial r}\right) = \frac{\partial C_d}{\partial t} \qquad (4)$$

with

if $t = 0$, $r > 0$ then $C_d=0$

if $t > 0$, $r = R$ then $C_d=C_d^*$ (5)

if $t > 0$, $r = 0$ then $\dfrac{\partial C_d}{\partial r} = 0$

Eq. (4) can easily be solved e.g. by the Laplace transform. Doing that and applying the surface renewal theory developed by Danckwerts [19], the mass transfer rate can be expressed as [7]:

$$J_d = \beta_d C_d^* \qquad (6)$$

where

$$\beta_d = \frac{D_d}{R}\left(\frac{\vartheta}{\tanh \vartheta} - 1\right) \qquad (7)$$

with

$$\vartheta = \sqrt{\frac{sR^2}{D_d}}$$

Note that the J_d value defined by Eq. (6) is an average value obtained by averaging by the exponential time distribution of the residence time of liquid elements and, accordingly, the particles in the boundary layer. It can easily be seen that the J_d value will be zero when the surface renewal frequency, s tend to zero, that is, the property of the boundary layer tends to the film theory.

Substituting the J_d ($J_d = \beta_d HC$) value into Eq. (1) and solving with boundary conditions (2), one can get as:

$$J = \sqrt{Ds}\,\frac{\psi}{\tanh(\lambda\psi)}C^* \qquad (8)$$

with

$$\psi = \sqrt{1 + \frac{\omega H}{1-\varepsilon}\frac{\beta_d}{s}}$$

Applying the surface renewal theory, one can get as:

$$J = \sqrt{Ds}\,\psi C^* \qquad (9)$$

2.1.3. Description of the Mass Transport in the Boundary Layer of a Nanofluid

As it was mentioned, the Brownian motion of suspended nanoparticles and the induced microscopic convection of the fluids around the nanoparticles are the most important contributing factor for enhancement of the mass transport in the boundary layer. The effect of this convection on the solute diffusion coefficient could be taken into account by an additional as e.g. dispersion term in a conductive model. The exact description of this process is not known yet. Assuming that the heat and mass transfer in the nanofluid are analogous to each other, the analytical approach for heat transfer in the nanofluid can be applied to describing mass transfer inside the nanofluid [23,29]. The general correlation for the heat transfer coefficient for the Brownian motion-induced Stokes flow of multiple nanoparticles can be given as [30]: $h = k_L(1 + A Re^m Pr^{0.333}\varepsilon)/R$ where A and m are constant. According to Prasher et al. [30] m=1.7. Accordingly, Nagy et al. [23] recommend the following equation in order to predict e solute diffusion coefficient in nanofluid, D_{nf}:

$$D_{nf} = D\left(1 + A\,Re^{1.7}\,Sc^{1/3}\left[\frac{\Delta y}{d}\right]^g\right)$$
$$\equiv D\left(1 + A\,Re^{1.7}\,Sc^{163}\left[\frac{\varepsilon^{1/3}}{1-\varepsilon^{1/3}}\right]^g\right) \qquad (10)$$

The g and A are constants. Xuan [29] suggests a more general equation for it as:

$$D_{nf} = D\left(1 + A\,Re_{nf}^m\,Sc_{nf}^n\,\varepsilon^p\right) \qquad (11)$$

The A, m, n, p are constants. According to Veilleux, and Coulombe [32] have found the following approach:

$$D_{nf} = D\xi Pe^2 \equiv D\xi\left(Re\,Sc\right)^2 \qquad (12)$$

where ξ is a constant.

Considering that the Δy distance lowers with the increase of the dispersed phase hold-up, Eq. (12) can be completed by factor $\Delta y/d$, as it is made in Eq. (10), one can get as:

$$D_{nf} = D\xi Pe^2 \equiv D\xi\left(Re\,Sc\right)^2\left[\frac{\Delta y}{d}\right]^g \qquad (12a)$$

For verification of the above equations the Eq. (10) and (12a) were used, because these expressions have got two parameters, only. On the other hand these equations are originated from different mass transfer approaches [23, 29, 32].

2.2. The Heterogeneous Model

The heterogeneous model takes into account the internal mass transport solving simultaneously the diffusion alternatively through the continuous and dispersed phases. This model is much complex than the homogeneous model. The first heterogeneous model was developed by Mehra [6] and Nagy [13-15]. Mehra [6] gives numerical solution while Nagy [13-15] developed analytical model and expresses the mass transfer rate by explicit, closed forms for the case when chemical reaction, in the continuous phase, namely biochemical reaction, is accompanied the absorption. The spherical particles were considered as cubic ones for simplification of the description (Fig. 1). It was investigated how the oxygen absorption rate is enhanced by the presence of dispersed organic phase. In order to be able to express the mass transfer rate, the differential mass balance equation system given for the continuous and the dispersed phases, should be solved. Applying the resistance-in-series model, it can give a rather complex equation system which is really difficult to be solved, analytically. Important advantage of the heterogeneous model is that it applicable for the case of fine, medium or large particles, as well. The set of differential mass balance equations for the heterogeneous model (for the heterogeneous part of the boundary layer; this is where particles are located in the diffusion path, behind each other, perpendicular to the gas-liquid interface to be solved will be as:

$$D_i\frac{\partial^2 C_i}{\partial y^2} = \frac{\partial C_i}{\partial t} \quad \text{i=continuous, d (disperse) phase (13)}$$
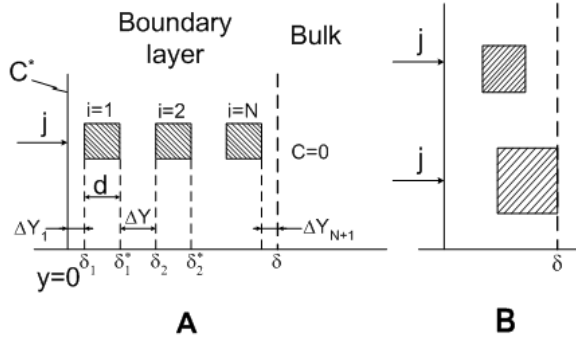
***Figure 1.** Illustration of the boundary layer for heterogeneous model*

The initial and boundary conditions, considering every internal interface between the cubic dispersed particles, is given by Eq. (14). The spherical particles are modeled by cubic one with the same volume). Thus, one can get the size of cubic particle: $d=d_p(\pi/6)^{1/3}$, the distance between cubic particles (the distance between the two interfaces of neighboring particles (see Fig. 1A), [13, 15]: $\Delta y=d(1/\varepsilon^{1/3}-1)$. The value of y_1 is the distance of cubic particle from the gas-liquid interface, perpendicular to the interface. The boundary conditions for the external interfaces, namely at $y=0$ and $y=\delta$, as well as for the internal interfaces of every sub-layer will be as (for details see Nagy, [13,14]:

if $t = 0$, $y > 0$ then $C=0$

if $t > 0$, $y = 0$ then $C=C^*$ (14)

if $t > 0$, $y = \delta_i$ and $y = \delta_i^*$ then $C_d=HC$

if $t > 0$, $y = \delta_i$ and $y = \delta_i^*$ then $D\dfrac{\partial C}{\partial y} = D_d \dfrac{\partial C_d}{\partial y}$

if $t > 0$, $y = \delta$ then $C=0$

Accordingly the differential equation system obtained contains $2N+1$ second-order differential equations. This equation system can be solved analytically, applying the Laplace transform. (The solution methodology is briefly summarized in the Appendix [34]). Look at the solution for cases given in Fig. 1. The mass transfer rate can be expressed as:

$$j = \beta C^* \quad (15)$$

The value of β, for the case of two sub-layers, i.e. when $y_1 + d \geq \delta$ (Fig. 1B) is expressed as:

$$\beta = \sqrt{Ds}\,\frac{\tanh(\vartheta_1)\tanh(\vartheta_d)+Hn}{\tanh(\vartheta_d)+Hn\tanh(\vartheta_1)} \quad (16)$$

where

$$\vartheta_1 = \sqrt{\frac{s\Delta y_1^2}{D}} = \lambda\Delta Y_1\,; \quad \vartheta_d = \sqrt{\frac{sd^2}{D_d}}\,; \qquad \lambda = \sqrt{\frac{s\delta^2}{D}}\,; \quad n = \sqrt{\frac{D_d}{D}}$$

The β value when one particle can only be located in the boundary layer, i.e. for the case when the boundary layer consists of three sub-layers ($y_1 + d+\Delta y_{N+1} = \delta$) (Fig. 1B), is as:

$$\beta=\sqrt{Ds}\,\frac{\tanh(\vartheta_1)\left[\dfrac{\tanh(\vartheta_d)}{nH}+\tanh(\vartheta_2)\right]+1+nH\tanh(\vartheta_2)\tanh(\vartheta_d)}{\dfrac{\tanh(\vartheta_d)}{nH}+\tanh(\vartheta_2)+\tanh(\vartheta_1)\left[1+nH\tanh(\vartheta_2)\tanh(\vartheta_d)\right]} \quad (17)$$

where

$$\vartheta_2 = \sqrt{\frac{s\delta^2}{D}}\Delta Y_{1+1}$$

Assuming that the film thickness is infinite, $\delta\to\infty$, according to the surface renewal theory, Eq. (17) can be rewritten as:

$$\beta=\sqrt{Ds}\,\frac{\tanh(\vartheta_1)\left[\dfrac{\tanh(\vartheta_d)}{nH}+1\right]+1+nH\tanh(\vartheta_d)}{\dfrac{\tanh(\vartheta_d)}{nH}+1+\tanh(\vartheta_1)\left[1+nH\tanh(\vartheta_d)\right]} \quad (18)$$

In the case of N particles in the boundary layer behind each other ($N>1$), the expression of the mass transfer rate needs to solve an algebraic equation system containing $2N$ equations where the N can be very large, especially, in the presence of fine particles in the boundary layer. This algebraic equation system obtained by the application of the boundary conditions expressed by Eq. (13) [13,14], solving it by the Cramer rules [34] enables to express the mass transfer rate. A brief description of this mathematical procedure is given in the Appendix. Accordingly, the mass transfer rate can be given as follows for that case:

$$\beta=\sqrt{Ds}\,\frac{\Psi_{A,N}+\Psi_{B,N}}{2\cosh(\vartheta_1)\Psi_{E,N}} \quad (19)$$

with

$$\Psi_{k,N} = \left(\tanh\vartheta_{N+1}+\frac{th\vartheta_d}{nH}\right)\Psi_{k,N-1}$$
$$+\left(n\tanh\vartheta_d\tanh\vartheta_{N+1}+\frac{1}{H}\right)\Omega_{k,N-1} \quad (20)$$

and

$$\Omega_{k,i} = \left(Hn\tanh\vartheta\tanh\vartheta_d+1\right)\Omega_{k,i-1}$$
$$+\left(Hn\tanh\vartheta+\frac{\tanh\vartheta_d}{n}\right)\Psi_{k,i-1} \qquad k=2,\dots N\text{-}1 \quad (21a)$$

$$\Psi_{k,i} = \left(n \tanh \vartheta_d + \frac{\tanh \vartheta}{H} \right) \Omega_{k,i-1}$$
$$+ \left(1 + \tanh \vartheta \frac{\tanh \vartheta_d}{nH} \right) \Psi_{k,i-1} \qquad k=2,\ldots N-1 \quad (21b)$$

where

$$\vartheta = \sqrt{\frac{s \Delta y}{D}} \equiv \lambda \Delta Y$$

with k=A,B,E

Not that according to the surface renewal theory δ is considered to be infinite. Modifying Eq. (20) accordingly, namely looking its limiting case when δ→∞ (consequently $\Delta Y_{N+1} \to \infty$), the $\psi_{j,N}$ value will be as:

$$\Psi_{k,N} = \left(1 + \frac{\tanh \vartheta_d}{nH} \right) \Psi_{k,N-1}$$
$$+ \left(n \tanh \vartheta_d + \frac{1}{H} \right) \Omega_{k,N-1} \qquad k=A,B,E \quad (22)$$

The starting values of $\Omega_{j,i}$ and $\Psi_{j,i}$ (j=A, B, E) are different from each other, which are as follows:

$$\Omega_{A,0} = H \exp(-\vartheta_1) \quad \Omega_{B,0} = H \exp(\vartheta_1) \quad \Omega_{E,0} = H \tanh(\vartheta_1) \ (23)$$

$$\psi_{A,0} = -\exp(-\vartheta_1) \quad \psi_{A,0} = \exp(\vartheta_1) \quad \psi_{A,0} = 1 \quad (24)$$

The j mass transfer rate can be given much easier for the film theory applying the resistance-in-series model. Thus, one can get, for the film theory, as:

$$j = \beta \left(C^* - C^o \right) \qquad (25)$$

where

$$\beta = \cfrac{1}{\cfrac{1}{\beta_1} + N \left(\cfrac{1}{\beta_d H} + \cfrac{1}{\beta_f} \right) + \cfrac{1}{\beta_{N+1}}} \qquad (26)$$

with

$$\beta_1 = \frac{D}{\Delta y_1}; \quad \beta_d = \frac{D_d}{d}; \quad \beta_f = \frac{D}{\Delta y}; \quad \beta_{N+1} = \frac{D}{\Delta y_{N+1}}$$

The overall mass transfer rate, related it to the total gas-liquid interface, can be given by the following equation [13,14]:

$$J = j\varepsilon^{2/3} + j^o \left(1 - \varepsilon^{2/3} \right) \qquad (27)$$

3. Results and Discussion

Several authors discussed the three-phase mass transfer rates applying both the homogeneous and the heterogeneous

models. This paper focuses to show which model can be recommended for application, depending on the particle size, the penetration depth and the surface renewal frequency. It is obvious that the penetration depth is crucially important using the heterogeneous model. Its value strongly depends on the residence time of the liquid element in the boundary layer. Accordingly, the number of particles that can alter the mass transfer rate can be very large, depending on the particle size, dispersed phase hold-up and surface renewal frequency. On the other hand, the applicability of the pseudo-homogeneous models should also depend on these parameters, as well. These circumstances were not really analyzed until yet because the heterogeneous model has got rather complicate mass transfer rate equations, though the particle/droplet size often grounds for its usage instead of the pseudo-homogeneous model.

3.1. Effect of the Particle Size

The mass transfer rate has been predicted applying every mass transfer models, namely pseudo-homogeneous models with finite particle diffusion rate [Eqs. (8) and (9)] and with instantaneous particle mass transfer [Eqs. (3a) and (3b)] as well as the heterogeneous model [Eqs. (19)-(24)] using the surface renewal theory. For every model the surface renewal theory is applied which means infinite thickness of the boundary layer. That means infinite number of particles behind each other perpendicular to the gas-liquid interface. As it was mentioned, the number of particle to be taken into account in our prediction is determined by the penetration depth, thus the N value can be calculated e.g. by equation of $\Delta y_p \approx \Delta y_1 + N(d + \Delta y)$. During calculation the N value can easily be estimated applying enough large N value for the calculation where its change does not cause further change in the j value. The effect of the particle size is illustrated in Fig. 2, at two different values of fluid mass transfer coefficient, namely $k_L = 1 \times 10^{-4}$ m/s and $k_L = 5 \times 10^{-4}$ m/s, as a typical figure. Accordingly the surface renewal frequency $(s = (k_L)^2/D)$ are 5 1/s and 125 1/s, as well as the penetration depth ($\Delta y_p = \sqrt{2Dt} \equiv \sqrt{2D/\beta}$ with the assumption of t=1/s) are 22.8 μm and 4.5 μm, respectively. Note that the enhancement is the ratio of the mass transfer rate in presence of dispersed phase related to that without dispersed phase. As it was shown [13-15], the distance between the first particle and the gas-liquid interface can strongly affect the j mass transfer rate. Its value was chosen to be 0.5Δy, which can be regarded as average value of the expectable ones from 0 up to Δy. The value of D was chosen to be 2×10^{-9} m²/s which is approximately equal to the diffusion coefficient of oxygen in water, and the solubility (H=10) is also close to the oxygen solubility in organic phase. The continuous lines give the enhancement (the mass transfer rate in three-phase system related to that without dispersed phase) at $k_L = 1 \times 10^{-4}$ m/s for instantaneous particle mass transfer rate (line 1), for finite particle mass transfer rate (line 2) and for the heterogeneous model (line 3).
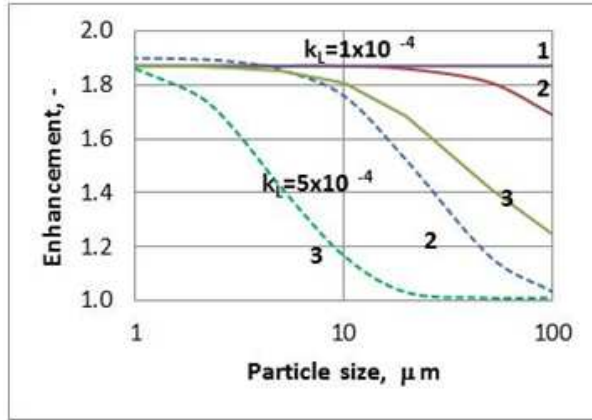
Figure 2. *The The enhancement as a function of the particle size applying the pseudo-homogeneous model with instantaneous particle mass transfer rate (lines 1), with finite mass transfer rate (lines 2) and the heterogeneous model (lines 3). ($D=2x10^{-9}$ m^2/s; $\varepsilon=0.2$; $D=D_d$; $H=10$; $\Delta y_1=0.5\Delta y$; $N=20-300$; continuous lines: $k_L=1x10^{-4}$ m/s; dotted lines: $k_L=5x10^{-4}$ m/s; line 1 is valid for both mass transfer coefficients)*

Figure 3. *The effect of the k_L mass transfer coefficient on the enhancement at different particles size in the liquid applying the pseudo-homogeneous model with instantaneous particle mass transfer rate (lines 1), with finite mass transfer rate (lines 2) and the heterogeneous model (lines 3). . ($D=2x10^{-9}$ m^2/s; $\varepsilon=0.2$; $D=D_d$; $H=10$; $\Delta y_1=0.5\Delta y$; $N=10-300$);*

For this k_L value, the two homogeneous models give the same enhancement up to about 20 μm particle size, indicating that the particle mass transfer rate can be really regarded as an instantaneous process. This is in harmony with the penetration depth obtained for that case. Note that the diffusion time of particles, t_d, with radius R can be estimated as $t_d=R^2/D$, and for the $t_d=d^2/D\approx1.62R/D$. Thus, the particle diffusion time for the heterogeneous model is about 62 % higher than that of a spherical particle. On the other hand the homogeneous model assumed that the concentration of the whole surface of particle is constant while it can strongly decrease with the increase of the particle size, thus, this model can overestimate the mass transfer rate at larger particle, i.e. if $d_p<<\delta$ inequality is not more fulfilled. The enhancement results of the heterogeneous model starts to deviate at about 3-5 μm from that of the homogeneous models. As it is expected the deviation of the models can be much higher when the mass transfer coefficient increases, i.e. when the residence time of liquid elements decreases (dotted lines in Fig. 3 with $k_L=5x10^{-4}$ m/s. Note that in the case of instantaneous internal mass transport the enhancement is not changed with the k_L mass transfer coefficient, thus, line 1 is also valid here). The about 25 times shorter residence time of liquid element in the boundary layer changes the shape of curves (dotted lines) much more dramatically than in case of $k_L=1x10^{-4}$ m/s. The question arises which model can be considered to be true, at higher particle size, in this case e.g. when $d_p>1$ μm. Up to about 5 μm, the internal transfer rate seems to be instantaneous. This can be true because the particle diffusion time and the residence time of the fluid elements are closely equal, namely 0.01 s, to each other. On the other hand the film thickness, it is about 4 μm, thus, it is obvious that the conditions for a pseudo-homogeneous model, namely that d_p should be much less than δ is not fulfilled at all. Accordingly the much lower results of the heterogeneous model should be more realistic than that of the homogeneous one.
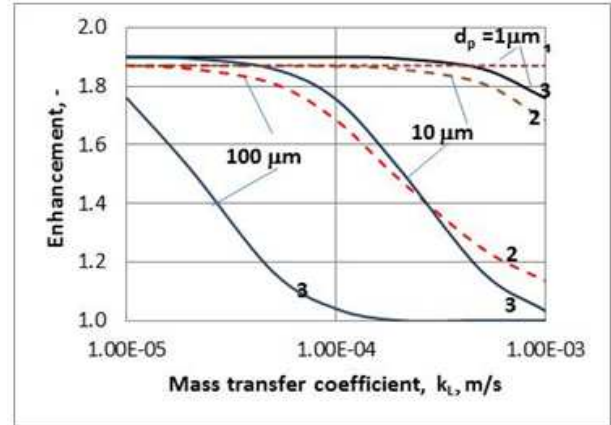
3.2. Effect of the k_L Mass Transfer Coefficient

The mass transfer coefficient of the poor liquid phase can also affect the applicability of the models at a given particle size as illustrated in Fig. 3 at three different particles sizes. The residence time ranges between 0.002 s to 20 s, while the diffusion depth between 1.12 μm up to 200 μm in the k_L range investigated. The enhancement for instantaneous internal mass transport is independent of the particle size, its value is equal 1.87. For values of $d_p< 1$ μm, the model with instantaneous mass transfer rate can be practically valid in the whole range of k_L investigated. The pseudo homogeneous model with finite internal reaction rate can be applied in the range where this model gives similar results with the heterogeneous one. That could also mean that if $d_p>1$ μm, the application of heterogeneous model might be recommended in the whole range of the k_L values. This figure shows clearly, that the effect of the dispersed phase strongly decreases with increase of the mass transfer coefficient, that is, with the decrease of the diffusion depth. Not that the distance of the first particle from the interface, Δy_1 was chosen to be $0.5\Delta y$, which means a relatively large value. Its effect is illustrated later, in Fig. 5.

3.3. Effect of the Particle Number, N, in the Diffusion Path

Every particle behind each other perpendicular to the gas-liquid interface, which is located in the penetration depth, can affect the mass transfer rate. Obviously, this effect lowers in the direction of the bulk phase. This situation is illustrated in Fig. 4 at different values of the liquid mass transfer coefficient without particles. As it is expected the number of particles which affects the enhancement is changing with the change of the k_L value. Even the 10th particle, though $d_p=10$ μm, increases the enhancement at $k_L=1x10^{-5}$ m/s. While at a high mass transfer coefficient, namely $k_L=1x10^{-4}$ m/s, the first two particles influences the mass transfer rate. On the other hand, the dispersed phase

has hardly any effect when the diffusion depth is less than the particle size. That the case when $k_L=5x10^{-4}$ m/s where $\Delta y_p \approx 4$ μm.

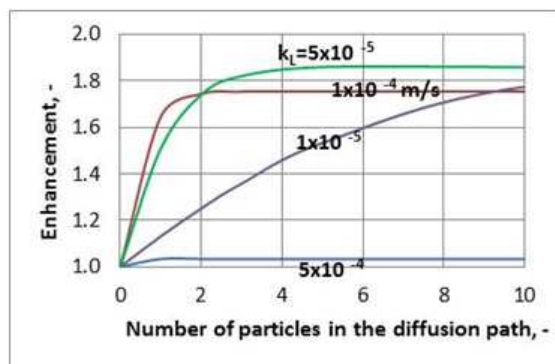**Figure 4.** *Effect of the particles in the diffusion path behind each other applying the heterogeneous model ($D=2x10^{-9}$ m²/s; ε=0.2; $D=D_d$; H=10; $\Delta y_1=0.5\Delta y$; $d_p=10$ μm)*

3.4. Effect of the H solubility coefficient

As it is expected the mass transfer rate increases with the increase of the H value (Fig. 5). The results of the homogeneous model will be identical due to the relatively small particle size chosen, $d_p=1$ μm (dotted line). The continuous lines give the enhancement when $\Delta y_1=0.5\Delta y$ ($\Delta y_1 \approx 0.35$ μm, line 2a), as it was done in the previous figures, as well as when the first particle is closer to the gas-liquid interface, namely $\Delta y_1=0.05\Delta y$, ($\Delta y_1 \approx 0.035$ μm, line 2b) in order to illustrate the importance of the Δy_1 value. As can be seen the difference between the two models increases with the increase of the H value (lines 1 and 2a). It should means to my opinion that the homogeneous model does not give real results at even small particle size when it has high solubility coefficient. On the other hand, if the first particle is located very close to the interface, the heterogeneous model gives higher enhancement than that of the homogeneous one. As it was mentioned the real average distance of the first particle from the interface could be the half of the distance between the particles as it was used during our previous calculations. It was also proved in previous papers that the solid particles can adhere to the gas-liquid interface [15, 35] creating multi-layer of particles on the interface. The mass transport through this multi layers can easily be calculated by the heterogeneous model presented here.

3.5. Mass Transfer into Nanofluid

For that case the internal mass transport can be really regarded as an instantaneous process. Thus the homogeneous model should give real results. According to Eqs. (10) to (12) the diffusion coefficient in a nanofluid can be increased by a multiplicative factor due to the particle Brownian motion induced microscopic convection of the fluids around the nanoparticles. Thus, the enhancement in nanofluid taking into account e.g. Eq. (3c) and Eqs. (10) to (12), can be expressed as:

$$E = \sqrt{\frac{D_{nf}}{D}} \qquad (28)$$

This means that with the increase of the diffusion coefficient in the nanofluid, the enhancement will be proportionally increased with the square of the diffusivities ratio.
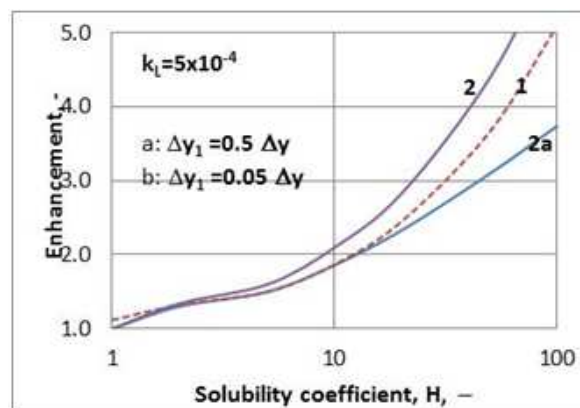

Figure 5. *The effect of the solubility of the dispersed phase on the enhancement [dotted line (line 1): homogeneous models; continuous lines (lines 2a, 2b): heterogeneous model] ($D=2x10^{-9}$ m²/s; ε=0.2; $D=D_d$; $d_p=1$ μm)*

3.6. Case Study

Because of its more and more importance in the chemical engineering, the effect of nanoparticles on the oxygen absorption rate was chosen for model verification. Thus, the measured data of Nagy et al. [23] as well as that of Olle et al. [22] were applied, who measured the absorption into nanofluid with dispersed n-hexadecane and with Fe_3O_4 nanoparticles covered by oleic acid, respectively. The particle size of n-hexadecane droplets was 65 nm, while that of the Fe_3O_4 nanoparticles was 20-25 nm, thus, the internal mass transfer rate can be regarded as instantaneous process and consequently, the pseudo-homogeneous models [e.g. Eq. (3b)] can be used. The enhancement can be predicted by Eq. (28). The diffusion coefficient in the nanofluid can be predicted by e.g. Eqs. (10) to (12a). The measured and the predicted data are shown in Fig. 6 in the case of oxygen absorption into n-hexadecane containing nanofluid. The dotted line represents the predicted data obtained by Eq. (10), while the continuous line that obtained by Eq. (12a). The values of the two parameters obtained are as: g=0.8, A=110 for Eq. (10), and g=0.8, ξ=0.016 for Eq. (12a). The agreement between the measured and the predicted data are good, data by Eq. (12a) give somewhat better results. Note that the g exponent was chosen to be the same in the both equations during estimation of its value. In a previous paper of Nagy et al. [23] the heterogeneous model suited also excellently the measured data.
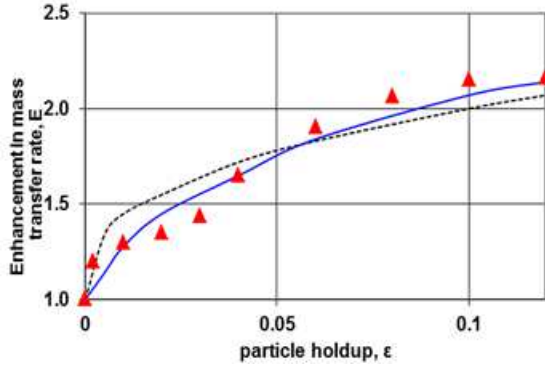
Figure 6. *Measured (Δ points) and the simulated curves using Eq. (10) [dotted line] and Eq. (12a) [continuous line] applying n-hexadecane dispersed phase (for details see [23], $d_p = 65$ nm, $k_L=1 \times 10^{-4}$ m/s, Re=0.039, Sc=435, H=8, D=D_p=2.3 x 10^{-9} m^2/s)*

The prediction of data of Olle et al. [22] seems to be more difficult. The application of Eq. (10) with g=1 did not give enough good agreement between the measured and the predicted data (see [23]) due to the high enhancement at low value of the particle holdup (ε=0.01). On the other hand, further increase of particle holdup does not give essential increase in the enhancement (Fig. 7, measured red squares). The predicted and measured data are in very good agreement. Values of constants, obtained, are: g= 0.3, ξ=0.01 for Eq.(12a), as well as g=0.3, A=25 for Eq. (10).
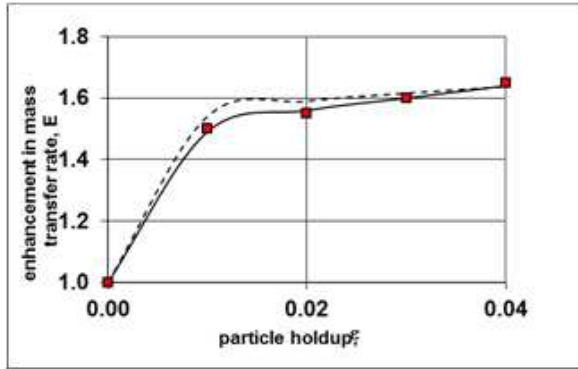

Figure 7. *Measured enhancement (black squares) taken from Olle et al. [22] and the predicted curves applying Eq. (10) [continuous line] and Eq. (12a) [dotted line] (d_p = 25 nm, Re=0.082, Sc=216, H=8, k_L=1 x 10^{-4} m/s, D=D_p=3.2 x 10^{-9} m/s)*

Comparing the value of constants obtained by the two particle sizes, it can be seen that values of all three parameters, g, A, ξ, are different. In principle, their values should be independent of the particle size. This should mean that the model equations can be regarded as approaches, thus, further investigations are needed to clarify the mass transport mechanism in nanofluid.

4. Conclusion

The absorption rate in the presence of nanosized or microsized dispersed phase was analyzed both theoretically and experimentally. Depending on the particle size different mathematical models should be applied for description of the mass transfer enhancement taking also into account the diffusion time (both the internal and external ones), the diffusion depth on the gas-liquid interface, etc. It was shown how the mass transfer rate is influenced by the k_L mass transfer coefficient, the number of particles in the diffusion path, the H solubility coefficient. In the case of nanosized particles the pseudo-homogeneous models while for microsized particles, depending on the residence time of the liquid elements, the heterogeneous model can be recommended. It was proved that the increased diffusion coefficient in nanofluid can be predicted by the dimensionless expressions given in this paper.

Acknowledgements

Appendix

Here we give a brief summary of the solution of the algebraic equation system, given by Eqs. (A1) to (A8) applying the boundary conditions given by Eqs. (13). For the solution of the determinants, the well-known Cramer rules were used.

The algebraic equation system, obtained by the boundary conditions, to be solved in order to get the values of A_i, B_i, E_i and F_i with i=1 to N+1 are as (see Fig. 1 for notations):

$$A_1 + B_1 = C^* \text{ at } Y=0 \tag{A1}$$

$$H\left\{ A_1 \exp\left(\lambda \frac{\delta_1}{\delta} \right) + B_1 \exp\left(-\lambda \frac{\delta_1}{\delta} \right) \right\} \\ = E_1 \exp\left(\lambda_d \frac{\delta_1}{\delta} \right) + F_1 \exp\left(-\lambda_d \frac{\delta_1}{\delta} \right) \quad \text{at } Y = \frac{\delta_1}{\delta} \tag{A2}$$

$$A_1 \exp\left(\lambda \frac{\delta_1}{\delta} \right) - B_1 \exp\left(-\lambda \frac{\delta_1}{\delta} \right) \\ = n\left\{ E_1 \exp\left(\lambda_d \frac{\delta_1}{\delta} \right) - F_1 \exp\left(-\lambda_d \frac{\delta_1}{\delta} \right) \right\} \quad \text{at } Y = \frac{\delta_1}{\delta} \tag{A3}$$

$$\vdots$$

$$H\left\{ A_i \exp\left(\lambda \frac{\delta_i}{\delta} \right) + B_i \exp\left(-\lambda \frac{\delta_i}{\delta} \right) \right\} \\ = E_i \exp\left(\lambda_d \frac{\delta_i}{\delta} \right) + F_i \exp\left(-\lambda_d \frac{\delta_i}{\delta} \right) \quad \text{at } Y = \frac{\delta_i}{\delta} \tag{A4}$$

$$A_i \exp\left(\lambda \frac{\delta_i}{\delta} \right) - B_i \exp\left(-\lambda \frac{\delta_i}{\delta} \right) \\ = n\left\{ E_i \exp\left(\lambda_d \frac{\delta_i}{\delta} \right) - F_i \exp\left(-\lambda_d \frac{\delta_i}{\delta} \right) \right\} \quad \text{at } Y = \frac{\delta_i}{\delta} \tag{A5}$$

$$\vdots$$

$$H\left\{A_N\exp\left(\lambda\frac{\delta_N^*}{\delta}\right)+B_N\exp\left(-\lambda\frac{\delta_N^*}{\delta}\right)\right\}$$
$$=E_N\exp\left(\lambda_d\frac{\delta_N^*}{\delta}\right)+F_N\exp\left(-\lambda_d\frac{\delta_N^*}{\delta}\right)\qquad \text{at } Y=\frac{\delta_N^*}{\delta}\quad\text{(A6)}$$

$$A_i\exp\left(\vartheta\frac{\delta_N^*}{\delta}\right)-B_i\exp\left(-\vartheta\frac{\delta_N^*}{\delta}\right)$$
$$=n\left\{E_i\exp\left(\vartheta_d\frac{\delta_N^*}{\delta}\right)-F_i\exp\left(-\vartheta_d\frac{\delta_N^*}{\delta}\right)\right\}\qquad \text{at } Y=\frac{\delta_N^*}{\delta}\quad\text{(A7)}$$

$$A_{N+1}\exp(\lambda)+B_{N+1}\exp(-\lambda)=0\qquad\text{at } Y=1\quad\text{(A8)}$$

with

$$\lambda=\sqrt{\frac{s\delta^2}{D}}\;;\qquad\qquad \lambda_d=\sqrt{\frac{s\delta^2}{D_d}}\;;$$

The values of parameters, A_i, B_i, E_i, F_i can be predicted by the following equation, applying the well known Cramer rules, as

$$\Psi_i=\frac{\mathcal{D}_{\Psi,i}}{\mathcal{D}}\qquad\text{where } \Psi=A, B, E, F\quad\text{and } i=1,..., N+1\quad\text{(A9)}$$

The knowledge of the values of A_i, B_i, E_i, F_i enable us to predict the concentration distribution in the boundary layer. But we only want to calculate the mass transfer rate through the boundary layer in presence of third, dispersed phase. It easy to get the expression of the mass transfer rate at Y=0, namely:

$$j=-\frac{D}{\delta}\lambda\left(A_1-B_1\right)\qquad\text{(A10)}$$

The determinants of the denominator and numerator of Eq. (A9), namely $\mathcal{D}_i$ and $\mathcal{D}$, can be obtained by the left hand side of Eqs. (A1) to (A8) after minor modifications. Chart A1 gives the $\mathcal{D}$ value. The determinant of $\mathcal{D}_{Ai}$ and $\mathcal{D}_{Bi}$ differ from Chart A1 in its first column, only. Thus, the first two columns of $\mathcal{D}_{Ai}$ and $\mathcal{D}_{Bi}$ can be given as:

$$\mathcal{D}_{A1}=2^{2N}\begin{bmatrix}H\exp(-\vartheta_1) & -1 & \\ -\exp(-\vartheta_1) & 0 & \\ & -\cosh(\vartheta_d) & \cdots \\ & -n\sinh(\vartheta_d) & \cdots \\ & \vdots\cdots & \end{bmatrix}$$

$$\mathcal{D}_{B1}=2^{2N}\begin{bmatrix}H\exp(\vartheta_1) & -1 & \\ \exp(\vartheta_1) & 0 & \\ & -\cosh(\vartheta_d) & \cdots \\ & -n\sinh(\vartheta_d) & \cdots \\ & \vdots\cdots & \end{bmatrix}$$

Chart A2. *The first two columns of the determinants to be given for determination of parameters A_1 and B_1.*

The solution of determinant, e.g. Chart 1, can be occurred by step by step reducing the number of rows and columns by unit in every step. Thus, e.g. it can be obtained for the value of $\mathcal{D}$ the following expression:

$$\mathcal{D}=2^{2N+1}\left(nH\right)^N\prod_{i=1}^{N+1}\cosh\vartheta_i^*$$
$$\prod_{i=1}^{N}\cosh\vartheta_{d,i}\left\{\Psi_{E,N}\tanh\vartheta_{N+1}+\Omega_{E,N}\right\}\qquad\text{(A11)}$$

where

$$\vartheta_i\equiv\vartheta\quad\text{when } i=2,\dots,N$$

$$\vartheta_{d,i}\equiv\vartheta_d\quad\text{with } i=1,\dots,N$$

The values of $\Psi_{E,N}$ and $\Omega_{E,N}$ can be calculated by Eqs. (14) to (16b). The values of $\mathcal{D}_{Ai}$ and $\mathcal{D}_{Bi}$ can similarly be got, and consequently the value of $A_1=\mathcal{D}_{A1}/\mathcal{D}$ and that of $B_1=\mathcal{D}_{B1}/\mathcal{D}$, as well.

$$\mathcal{D}=2^{2N+1}\begin{bmatrix}-H\sinh(\vartheta_1) & -1 & 0 & & & & & & \\ -\cosh(\vartheta_1) & 0 & n & & & & & & \\ & -\cosh(\vartheta_d) & \sinh(\vartheta_d) & H & 0 & & & & \\ & -n\sinh(\vartheta_d) & n\cosh(\vartheta_d) & 0 & -1 & & & & \\ & & & H\cosh(\vartheta) & -H\sinh(\vartheta) & -1 & 0 & & \\ & & & \sinh(\vartheta) & -\cosh(\vartheta) & 0 & n & & \\ & & & \vdots & & & \vdots & \cdots & \\ & & & & & -\cosh(\vartheta_d) & \sinh(\vartheta_d) & H & 0 \\ & & & & & -n\sinh(\vartheta_d) & n\cosh(\vartheta_d) & 0 & -1 \\ & & & & & & & -\cosh(\vartheta_{N+1}) & -\sinh(\vartheta_{N+1})\end{bmatrix}$$

Chart 1. *Determinant of Eq. (A9)*

Nomenclature

C	concentration of the absorbed component in the liquid phase, mol/m^3
C*	concentration of the absorbed component at the gas-liquid interface, at $y=0$, mol/m^3
d	diffusion distance within the cubic particles, m
d$_p$	particle size, m
D	diffusion coefficient in the continuous phase, m^2/s
D$_d$	diffusion coefficient in the dispersed phase, m^2/s
D$_{nf}$	enhanced diffusion coefficient in the nanofluid, m^2/s
E	enhancement (=J/J^o)
H	solubility (partition) coefficient of the absorbed component between dispersed phase and continuous one (=C$_d$/C)
j	partial mass transfer rate, mol/m^{2}s
J^o	mass transfer rate without dispersed phase, mol/m^{2}s
J	overall mass transfer rate with dispersed phase, mol/m^{2}s
k$_L$	gas-liquid mass transfer coefficient without particles, (e.g. $=\sqrt{Ds}$), m/s
N	number of particles in the boundary layer, behind each other, perpendicular to the gas-liquid interface, -
Pr	Prandtl number, -
R	particle radius, m
Re	Reynolds number of Brownian nanoparticles, -
s	surface renewal frequency, l/s
Sc	Schmidt number, -
T	temperature, K
v	connective velocity of Brownian nanoparticles, m/s
y$_1$	distance of the first particle from the gas-liquid interface, m
Δy	distance between the cubic particles, m
Δy_{N+1}	width of the last sub-layer, m

Greek letters

β	physical mass transfer coefficient in presence of particles, m/s
δ	film thickness, m
ϵ	hold-up of dispersed phase

Subscripts

d	dispersed phase
p	particle

References

[1]   P.A. Ramachanran, Gas Absorption in slurries containing fine particles: review of models and recent advances, Ind. Eng. Chem. Res., vol. 46, 2007, pp**.** 3137-3152;

[2]   R. Kaur, M, Ramakrishna, K.D.P. Nigam, Role of dispersed phase in gas-liquid reactions: a review, Reviews in Chemical Engineering., vol. 23, 2007, pp. 247-300;

[3]   E. Dumont, and H. Delmas, Mass transfer enhancement of gas absorption in oil-in-water systems: a review, Chem. Eng. Processing, vol. 42, 2003, pp. 419-438;

[4]   W.J. Bruining, G.E.H. Joosten, A.A.C.M. Beenackers and H. Hofman, Enhancement of gas-liquid mass transfer by a dispersed second liquid phase, Chem. Eng. Sci., vol. 41, 1986, pp. 1973-1877;

[5]   R.D. Holsvoogd, W.P.M. van Swaaij and L.L. van Dierendonck, The absorption of gases in aqueous activated carbon slurries enhanced by absorbing or catalyst particles, Chem. Eng. Sci., vol. 43, 1988, pp. 2181-2187;

[6]   A. Mehra, Heterogeneous modeling of gas absorption in emulsions, Ind. Eng. Chem. Res., vol. 38, 1999, pp. 2460-2468;

[7]   E. Nagy, and A. Moser, Three-phase mass transfer: improved pseudo-homogeneous model. AIChEJ .vol. 41, 1995, pp. 23-34;

[8]   A. Lekhal, R.V. Chaudhari, A.M. Wilhelm and H. Delmas, Mass transfer effects on hydrofomylation catalyzed by a water soluble complex, Catalysis Today, vol. 48, 1999, pp. 265-272;

[9]   G.D. Zhang, W.F. Cai, C.J. Xu and M. Zhou, A general enhancement factor model of the physical absorption of gases in multiphase systems, Chem. Eng. Sci., vol. 61, 2006, pp. 558-568;

[10] D.W.F. Brilman, W.P.M. van Swaaij and G.F. Versteeg, A one dimensional instationary heterogeneous mass transfer model for gas absorption in multiphase systems, Chem. Eng. Proc., vol. 37, (6), 1988, pp. 471-488;

[11] B.H. Junker, D.I.C. Wang, and T.A. Hatton, Oxygen transfer enhancement in aqueous/perfluorocarbon fermentation systems: II. Theoretical analysis, Biotechnol. Bioeng., vol. 35, 1999, pp. 586-597;

[12] C.J. van Ede, R. van Houten, and A.A.C.M. Beenackers, Enhancement of gas to water mass transfer rates by dispersed organic phase, Chem. Eng. Sci., vol. 50, (18), 1995, pp. 2911-2922;

[13] E. Nagy, Three-phase mass transfer: one-dimensional heterogeneous model, Chem. Eng. Sci. vol. 50, 1995, pp. 827-836;

[14] E. Nagy, Heterogeneous model for a number of particles in the diffusion path, Hung. J. Ind. Chem. vol. 26, 1998, pp. 229-240;

[15] E. Nagy, On the three-phase mass transfer with solid particles adhered to the gas-liquid interface, Central European Journal of Chemistry vol. 2, 2003, pp. 160-177;

[16]   D.W.F. Brilman, M.J.V. Goldschmidt, G.F. Versteeg, and W.P.M. van Swaaij, Heterogeneous mass transfer models for gas absorption in multiphase systems, Chem. Eng. Sci., vol. 55, 2000, pp. 2793-2812;

[17] C. Lin, M. Zhou, and C.J. Xu, Axisymmetrical two-dimensional heterogeneous mass transfer model for the absorption of gas into liquid-liquid dispersion, Chem. Eng. Sci., vol. 45, 1999, pp. 389-399;

[18] Sh. Shen, Y. Ma, S. Lu, and Ch. Zhu, A one-dimensional unstable heterogeneous mass transfer model for gas

absorption enhancement by third dispersed phase droplet, Chinese J. Chem. Eng., vol. 17 2009, pp. 602-607;

[19] Dankwerts, P.V. Gas-Liquid Reactions; McGraw-Hill, New York, 1970

[20] A. Kaya, A. Schumpe, Surfactant adsorption rather than "shuttle effect"? Chem. Eng. Sci. vol. 60, 2005, pp. 6504-6510;

[21] V. Linek, M. Kordac, M. Soni, Mechanism of gas absorption enhancement in presence of fine solid particles in mechanically agitated gas-liquid dispersion. Effect of molecular diffusivity, Chem. Eng. Sci. vol. 63, 2008, pp. 5120-5128;

[22] B. Olle, S. Bucak, T.C. Holmes, L. Bromberg, A. Hatton, D.I.C. Wang, Enhancement of oxygen transfer using funcionalized magnetic nanoparticles, Ind. Eng. Chem. Res. vol. 45, 2006, pp. 4355-4363;

[23] E. Nagy, T. Feczkó, B. Koroknai, Enhancement of oxygen transfer rate in the presence of nanosized particles, Chem. Eng. Sci., vol. 62, 2007, pp. 7391-7398;

[24] S. Komati, A. K. Suresh, Anomalous enhancement of interphase transport rates by nanoparticles: effect of magnetic iron oxide on gas-liquid mass transfer, Ind. Eng. Chem. Res. vol. 49, 2010, pp. 390-405;

[25] S. Komati, A.K. Suresh, CO_2 absorption into amine solutions: a novel strategy for intensification based on the addition of ferrofluids, J. Chem. Technol. Biotechnol. vol. 83, 2006, pp. 1094-2001;

[26] J.K. Kim, J.Y. Jung, Y.T. Kang, The effect of nano-particles on the bubble absorption performance in a binary nanofluid,

Int. J. Refrigeration, vol. 29, 2006, pp. 22- 28;

[27] S. Krisnamurthy, P., Bhattachaya, P.E., Phelan, Enhanced mass transport in nanofluids, Nanoletters, vol. 6, 2006, pp. 419-423;

[28] X. Fang, X. Yimin, Q. Li, Experimental investigation on enhanced mass transfer in nanofluids, Appl. Physic Letters, vol. 95, 2009, pp. 203108-11

[29] Y. Xuan, Conception for enhanced mass transport in binary nanofluids, Heat Mass Transfer, vol. 46, 2009, pp. 277-279;

[30] R. Prasher, P. Bhattacharya, P. E. Phelan, Brownian-motion-based convective-conductive model for th effective thermal conductivity of nanofluids, Transaction of ASME, vol. 128, 2006, pp. 588-595;

[31] J. Veilleux, S. Coulombe, A dispersion model of enhanced mass diffusion in nanofluids, Chem. Eng. Sci., vol. 66, 2011, pp. 2377-2384;

[32] J. Veilleux, S. Coulombe, A total internal reflection fluorescence microscopy study of mass diffusion enhancement in water-based alumina nanofluids, J. Appl. Physics, vol. 108, 2010, pp. 104316-24;

[33] E. Nagy: Mass transfer through a dense, polymeric, catalytic membrane layer with dispersed catalyst, Ind. Eng. Chem. Res. vol. 46, 2007, pp. 2295-2306;

[34] E. Nagy, Basic equations of mass transport through a membrane layer, Elsevier, New York, 2011

[35] J.P Demmink, A. Mehra, A.A.C.M. Beenackers, Gas absorption in the presence of particles showing interfacial affinity: case of fine sulphur precipitations, Chem. Eng. Sci., vol. 53, 1998, pp. 2885-2902.